Numerical Modelling of Covers and Slabs Subject to Seasonal Surface Suction Variations

J. Li
PhD student
School of Civil Engineering, University of South Australia
D.A. Cameron
Senior Lecturer, School of Civil Engineering, University of South Australia
K.G. Mills
Senior Lecturer, School of Civil Engineering, University of South Australia

Summary This paper presents a moisture (suction) flow-soil-footing interaction model for the analysis of a stiffened slab resting on an expansive soil, which is subject to seasonal surface suction variations at the edge of the slab. The model is formulated using the finite element program, MSC/NASTRAN. The transient flow of moisture and the deformation of the soil have been simulated using a thermo-mechanical analogy. Both side friction and lateral swelling pressures against beams are considered in the model.

1. INTRODUCTION

Current methods for the design of footings on expansive soils are based on many simplifying assumptions. For example, the analysis is usually carried out by considering the interaction of a loaded footing superimposed on a pre-formed, cylindrical, free soil mound (centre or edge heave). In this approach, the mound shape has to be initially estimated and there exists a considerable degree of uncertainty. In the field, however, the soil mound develops with the footing in place. The size and shape of the mound depend on many factors including the geometry, size and stiffness of the footing, the location and magnitude of loads, as well as the long term and seasonal changes in the soil suction profile. In addition, side shears and lateral swelling pressures act on any embedded beams, yet these tractions are ignored in conventional analysis of the soil-footing interaction.

This paper presents a moisture (suction) flow-soil-footing interaction model for analysis of a stiffened slab resting on an expansive soil foundation, which is undergoing swelling and shrinkage. The environmental conditions assumed are typical of the semi-arid areas of southern Australia. The model is incorporated in the finite element program MSC/NASTRAN. The assumption of superposition and the estimation of initial mound shape are avoided. Movements of the foundation and the footing are generated by the initial soil suction conditions and subsequent changes in the boundary conditions. A variety of complex factors may be taken into account such as multi-dimensional transient moisture flow, multi-dimensional swelling, skin friction and suction-dependent soil parameters.

2. THEORY AND NUMERICAL MODEL

2.1 The Governing Equation for Moisture Diffusion in Expansive Soil

Flow of moisture in unsaturated soil is a complicated phenomenon. Moisture will flow through permeable, continuous soil layers by diffusion from a region of low suction to a region of high suction. In reality, cracks and fissures which exist in the soil structure will permit moisture to flow more readily throughout the body of soil.

The flow of water through a uniform soil mass can be described using Darcy's law:

$$v_i = -k_{ij} \frac{\partial \psi}{\partial x_j} \qquad (1)$$

where v_i = velocity of flow, k_{ij} = coefficient of permeability (or hydraulic conductivity), $\partial\psi/\partial x_j$ = gradient of flow potential or total head, ψ, in the x_j direction.

Darcy's law, which was originally derived for saturated soil, can equally be applied to the flow of water through an unsaturated soil. The only difference is that for flow through an unsaturated soil, the coefficient of permeability, k, is no longer a constant but is a function of the suction of the soil (Richards, 1967).

Through the application of Darcy's law and equations of continuity of moisture flow, the following diffusion equation can be obtained to describe the unsaturated moisture flow (Richards, 1967; Lytton, 1977)

$$\frac{\partial u}{\partial t} = \frac{\partial u}{\partial \theta} \frac{\partial}{\partial x_i} (k_{ij} \frac{\partial \psi}{\partial x_j}) \qquad (2)$$

The convention of summation on repeated indices is used in the above equation. The term, $\partial u/\partial\theta$, is the slope of the curve which relates suction to the volumetric water content, θ. For many soils, and especially expansive soils, the variable $\partial u/\partial\theta$ can be assumed to be relatively constant over the range considered (Richards, 1967).

The total flow potential, ψ, in expansive soils is made up of total suction potential, u, the gravitational potential, x_3, and the overburden potential, Ω (Lytton, 1977):

$$\psi = -u + x_3 \pm \Omega \tag{3}$$

It has been shown (Sokolov and Amir, 1973) that the gravitational potential and the overburden potential nearly cancel each other and the small difference between them is usually negligible relative to the suction potential. Since the primary purpose herein is to evaluate soil movements due to soil suction change, only the suction potential in equation (2) needs to be considered. Therefore ψ becomes equivalent to the suction potential.

If the soil body is assumed to be homogeneous and isotropic, the governing differential equation (2) can be simplified (Mitchell 1980)to:

$$\frac{\partial^2 u}{\partial^2 x} + \frac{\partial^2 u}{\partial^2 y} + \frac{\partial^2 u}{\partial^2 z} = \frac{1}{\alpha}\frac{\partial u}{\partial t} \tag{4}$$

where $\alpha = k/(c\,\rho_d)$ = diffusion coefficient,
ρ_d = dry density
and c = the moisture characteristic.

When the total suction, u, is substituted by temperature, T, equation (2) or (4) becomes the well-known heat diffusion equation, which governs heat transfer in solids. Thus the transient diffusion of soil suction can be solved in two or three dimensions and is unconstrained by the nature of the boundary conditions. The analogy between heat and moisture diffusion due to soil suctions has been described elsewhere (Li *et al*, 1995b).

In MSC/NASTRAN finite element program, both transient and steady state moisture diffusion can be modelled. The unsaturated permeability may be a function of suction (suction-dependent), location (non-homogeneous), and/or direction (anisotropic). The validity of the thermal analogy was verified by comparing solutions with known theoretical solutions and laboratory experimental results.

2.2 Boundary Conditions

Generally, three types of boundary condition may be considered:

a) the Dirichlet - type, where suction u (t) is prescribed,
b) the Neumann - type, where the gradient q of u(t) is given,
c) mixed-type conditions, (a) and (b).

A no-flow boundary condition is analogous to a heat insulated boundary and can be analysed mathematically by assuming q = 0 in (b). A convection boundary condition, which represents moisture exchange between the soil mass and the atmosphere, is an example of the third kind of boundary condition. More information about boundary conditions can be found in Li *et al* (1995b). Boundary conditions (a) and (b) have been considered in this paper. Alternative boundary conditions have not been taken into account here due to the lack of supporting field data.

The surface of the soil that is not covered by the slab is subjected to seasonal variations of moisture. Moisture changes are gradual under the slab, resulting in time dependent soil and slab movements. It has been shown (Mitchell 1980) that surface suction can be assumed to vary in a sinusoidal manner in response to climate cycles as follows:

$$u(0, t) = U_e + U_0 \cos(2n\pi t - p) \tag{5}$$

where U_e = equilibrium suction (pF)
U_0 = amplitude of the suction wave (maxm. suction change) at the ground surface (pF)
n = climatic frequency (cycle/year)
p = phase angle
t = the time variable.

It should be pointed out that the sinusoidal function of time is only an approximation of the soil surface moisture variation throughout the year. Nevertheless, it is an acceptable approximation for semi-arid, seasonal moisture variations.

The climate of Adelaide, South Australia, is semi-arid with a relatively dry period from October to April and a wet period from May to September. Figure 1 shows near-surface suction data taken from a Northern Adelaide suburb. The soil suction changes generally follow rainfall and evaporation patterns for the area.

The surface boundary condition used in the numerical model is also given in Figure 1. This theoretical curve fits the field measured data reasonably well and is considered appropriate for most of Adelaide. However, a different surface boundary condition can be expected for other sites where the weather and drainage conditions are substantially different to the conditions at the site from which the data were obtained.

In addition to seasonal climate variation, there are many other environmental factors affecting expansive soil volume change. An event such as lawn watering, wetting due to leaking underground services or drying caused by trees can be modelled by the thermal analogy, but will not be discussed in this paper.

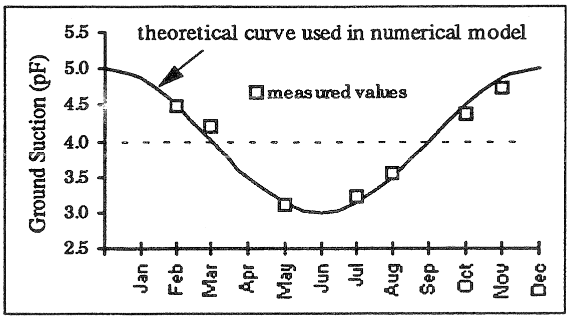

Figure 1. Surface Suction Variation with Time

2.3 Deformations in Expansive Soil

Expansive soil behaviour is affected by changes in soil suction, as well as external loading due to footing self-weight and structural loads. A stress-strain relationship for expansive soil can be written as follows (Li *et al*, 1995a):

$$\{\sigma\} = [D_e(u)]\,(\{\varepsilon\} - \{\varepsilon_{swell}\}) \qquad (6)$$

where $\{\sigma\}$ and $\{\varepsilon\}$ are the stress and strain vector respectively, and $[D_e(u)]$ is the suction dependent elasticity matrix. $\{\varepsilon_{swell}\}$ is the strain induced by the suction change.

The swelling forces at nodes are determined as follows:

$$\{Q\}_{SF} = \int [B]^T [D_e]\,\{\varepsilon_{swell}\}\,dV_{el} \qquad (7)$$

where $\{Q\}_{SF}$ is the swelling force vector, $[D_e]$ is the elastic matrix for the element, $[B]$ is called the strain-displacement matrix.

In NASTRAN finite element analysis, the soil response to changes in suction and stress conditions may be assumed to be anisotropic elastic, non-linear elastic or elastic-plastic, with the Mohr-Coulomb shear strength law as the plastic failure criterion.

3. APPLICATION OF THE MODEL

A stiffened slab on expansive soil was analysed in two dimensions as shown in Figure 2. The depth of all three stiffening beams varied from 0 to 1.2 m to investigate the effect on the suction distribution beneath the slab and the performance of the footing.

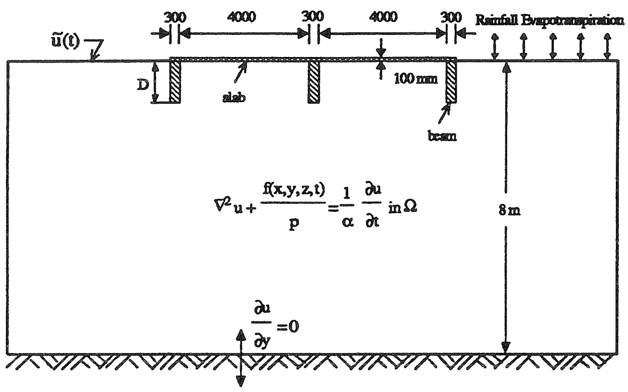

Figure 2. Two-Dimensional Foundation-Footing System with Boundary Conditions

Loading conditions representative of a single storey brick veneer dwelling were used in this investigation. The self-weight of the concrete footing was included automatically.

After considering the shrinkage cracks, fissures and slickensides that may be present in the field, the coefficient of diffusion was taken to be 5.8 x 10^{-4} cm^2/sec, ten times the value obtained from laboratory evaporation testing of a black earth clay.

The elastic modulus of the soil was taken as 40 MPa and Poisson's ratio as 0.2. Vertical and horizontal instability indices, I_{pty} and I_{ptx}, were assumed to be 4%/pF and 2%/pF respectively. Soil concrete interfaces were modelled with interface elements having a shear stiffness and a friction coefficient of 300N/mm and 1.0, respectively. These values were based on modified shear box testing of composite black earth clay/concrete specimens.

The initial suction profile at the boundaries was assumed to be at the equilibrium state, having a constant suction value of 4pF. The phase angle, p, was taken as 270°, which implied that the slab was constructed at the end of the wet season.

Case one - D = 0m

In the first case analysed, the footing consisted of a slab without any stiffening beams. The calculated soil suction profiles at different positions about the slab are plotted in Figure 3. The soil suction profile varied in a cyclical manner with full seasonal change at the open field and a reduced seasonal change at the edge of the slab. The maximum change in surface suction at the edge of the slab was only half that which occurred at the uncovered surface. Obviously this reduction was due to the effect of the surface slab cover.

The depth of seasonal moisture variation was 1.9m, based on a maximum variation of suction at depth of 0.2 pF. No change in suction occurred beneath the centre of the slab since the initial condition assumed here was equivalent to the equilibrium suction, U_e.

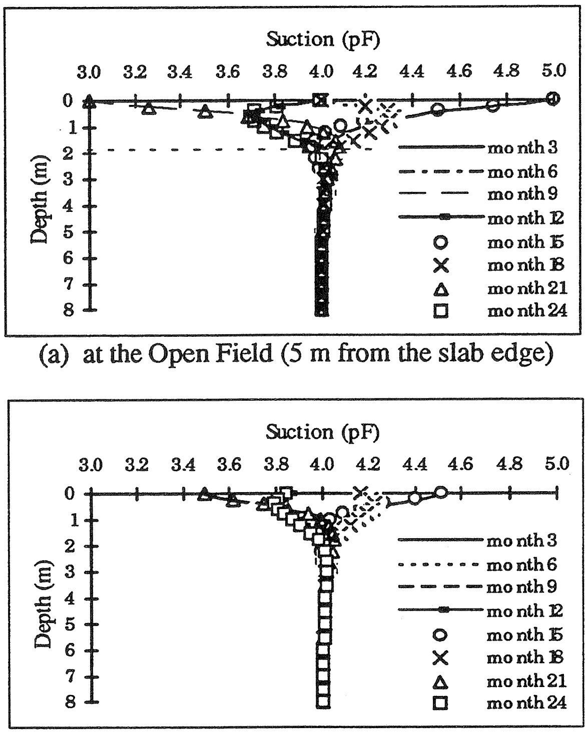

(a) at the Open Field (5 m from the slab edge)

(b) at the Edge of the Slab

Figure 3. Suction Profiles at Different Positions

A special sub-case of case 1 was studied by removing all loads and taking away the stiffness of the concrete slab. The influence of a surface cover in producing free soil mound shapes could then be explored. In particular, the edge distance, e, which is such a critical design parameter and is very difficult to estimate (Wray, 1980), may be evaluated.

Figure 4 illustrates the variation of suction at the surface with time below the cover at different distances from its edge. The changes in suction quickly decreased as the edge distance increased. Almost no suction change occurred under the cover at a distance of 1.7 m from its edge.

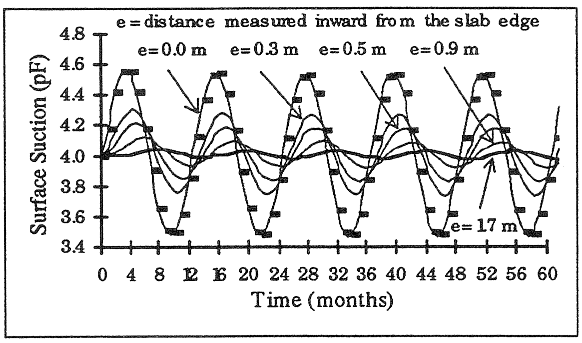

Figure 4. Calculated Surface Suction Variation at Different Edge Distances

A design edge distance, e of 0.9m may be inferred from the data, based on a maximum suction variation of 0.2pF.

Seasonal suction variation and the corresponding soil movements at various depths, D, in the open field are shown in Figures 5 and 6 respectively. The soil movement exhibited a time-lag of about one month behind the periodic suction variation. Both suction changes and soil movements decreased with depth. There was also an increasing time lag with increasing depth, a phenomenon confirmed by previous monitoring in Adelaide of seasonal soil movement (Aitchison and Holmes, 1953).

Figure 7 illustrates soil movement beneath the cover with respect to the movement occurring around the perimeter and outside the cover. The characteristic surface ground movement, y_s, (AS2870) was determined to be 71mm. The differential movement across the flexible cover, y_m, for the centre heave (edge shrinkage) and the edge heave were 26 and 20mm respectively.

The edge and centre movements of the loaded slab, and the open field surface movement are plotted with respect to time in Figure 8. All movements were cyclical with the climate, but the maximum edge and centre displacements of the slab lagged behind the displacement of the soil surface by one and six months respectively. Although the edges of the slab moved up and down with the seasons, there was no significant movement at the centre of the slab, for reasons previously discussed.

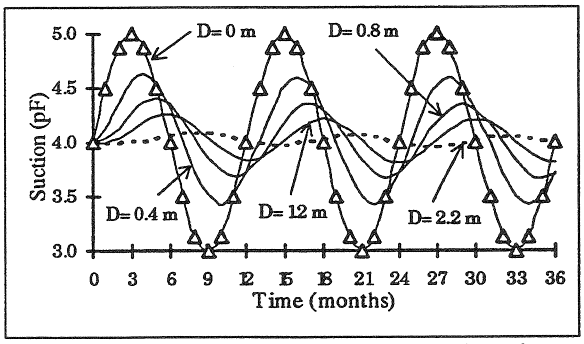

Figure 5. Seasonal Suction Variation with Time (Open Field)

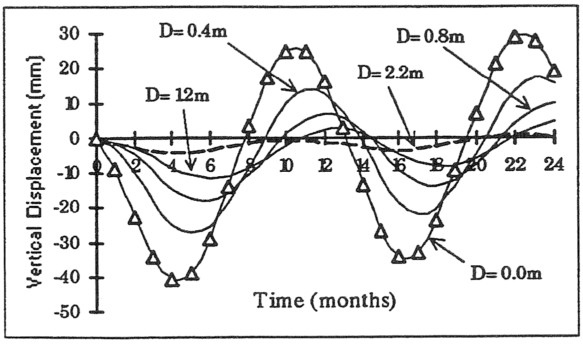

Figure 6. Seasonal Soil Movements (Open Field)

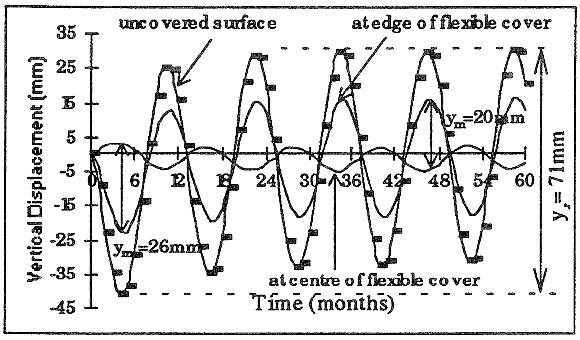

Figure 7. Seasonal Surface Movements at Various Locations about a Cover

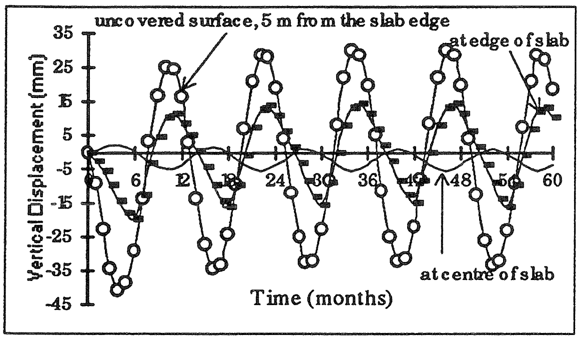

Figure 8. Seasonal Surface Movements at Open Field and at the Edge and the Centre of the Slab

The distortion patterns of the impermeable cover and the loaded slab were compared month-by-month over a period of ten years. Examples are shown in Figure 9. It is interesting to note that the values of the differential movement across the flexible cover (y_m) at Month 4 and Month 6 were 26 and 20 mm respectively, but the deflection ratio of the slab (Δ/L) at Month 6 was 20% larger than that at Month 4.

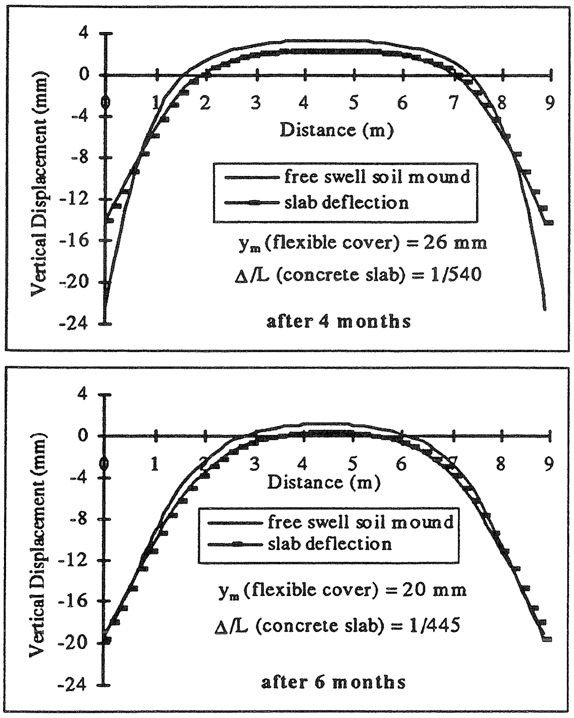

Figure 9. Cover and Slab Distortions

Therefore mound shape is more significant than mound height in influencing the performance of this relatively flexible slab.

During mound development, a part of the slab may become detached from the ground and act as a cantilever, leading to redistribution of foundation pressure and possibly slab cracking. The location of slab separation is clearly illustrated in Figure 9. Edge lift-off of 8mm occurred at Month 4, together with an edge lift-off distance of about 0.7m. The maximum concrete tensile stress was not exceeded.

Case two - D = 0.6 m

In case two, the depth of the stiffening beams was 0.6m. Figure 10 provides soil suction profiles just outside the slab, both at and inside the edge beam. The edge beam effectively restricts moisture flow.

The vertical displacement of the slab and the uncovered surface is plotted in Figure 11. Typical deformed shapes of the slab and the foundation (deflection magnified by ten) are shown in Figure 12. At year 9, the footing moved up due to soil swelling, but this upward displacement trend was reduced by the embedded beams, and especially by the centre beam. The skin friction on the beam acted in the opposite direction to the slab movement, and therefore reduced the deflection.

After 9.5 years, the edge beams tended to tilt inwards (1/130) due to the unequal horizontal soil pressures on either side of the beam. Soil had separated from the outside of the beam but was in close contact on the inside.

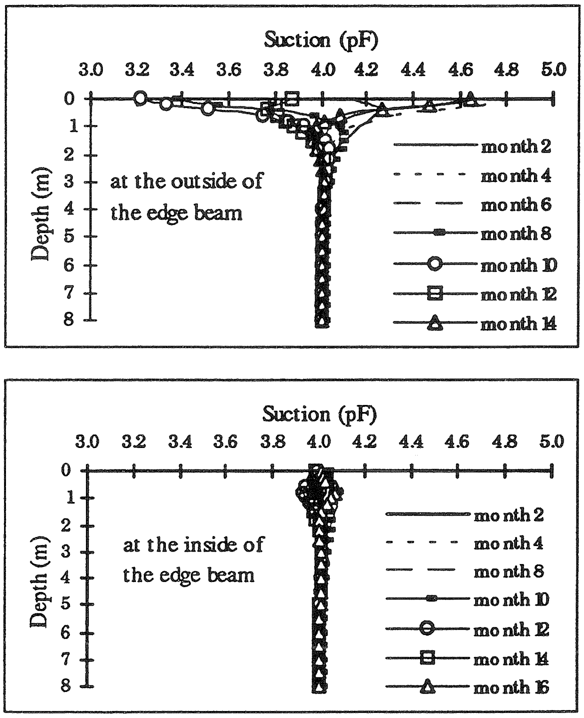

Figure 10. Suction Profiles about the Edge Beam

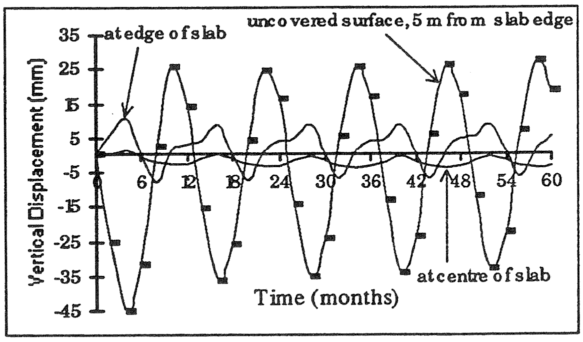

Figure 11. Calculated Vertical Displacement of Slab and Uncovered Surface (D= 0.6 m)

Other Cases

More complicated cases have been investigated. Initially dry sites, deeper beams and anisotropic permeability have been explored. Parametric studies of the effect of footing stiffness, loading, soil modulus and reactivity on the performance of slabs were also conducted. Results will be presented elsewhere.

4. CONCLUSIONS

A thermo-mechanical model has been presented for the study of covers and slabs subject to seasonal surface suction variations. The numerical model can provide the following information:

- the depth of seasonal moisture variation.
- the edge distance parameter.
- the suction distribution within the foundation at any time for the given boundary conditions.
- the soil free mound shape as a function of time.
- the deflections and stresses of the footing as a function of time.

The results of the parametric studies indicated that the skin friction and lateral swelling pressures acting on the embedded beams have a significant influence on the patterns of the slab deflections.

The paper has demonstrated the usefulness of a thermal analogy of moisture diffusion and soil deformation processes in understanding the patterns of movement of expansive clay soil. Further research is needed to calibrate the numerical model with field data.

5. REFERENCES

Aitchison, G.D. and Holmes, J.W. (1953), 'Aspects of Swelling in the Soil Profile', *Australian Journal of Applied Science*, Vol. 4, pp. 244-259.

Li, J., Cameron D.A., Bayetto, P.M. and Goldfinch, J.C. (1995a), 'Field Study and Back-analysis of a Concrete Slab Footing on Expansive Soils', *Civil Eng. Trans. I.E.Aust.*, Vol CE37, No.1, pp. 21-27.

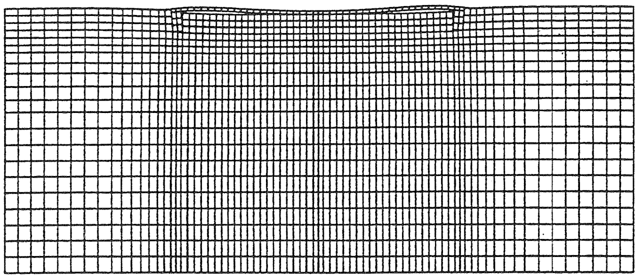

(a) After 9 years

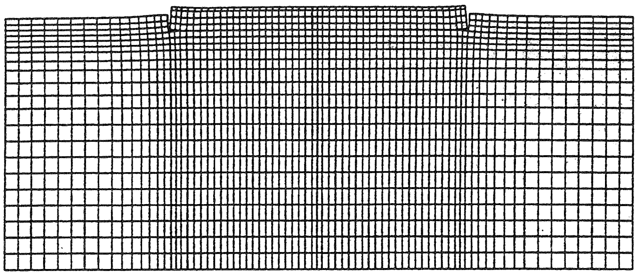

(b) After 9 years and 6 months

Figure 12. Deformed Shapes of the Footing and the Foundation

Li, J, and Cameron, D.A. (1995b), 'Finite Element Analysis of Deep Beam in Expansive Clays', *First International Conference on Unsaturated Soils*, Paris, France, September, 1995, pp. 1109-1115.

Lytton, R.L. (1977), 'Foundation in Expansive Soils', Ch. 13, *Numerical Methods in Geotechnical Engineering*, C.S. Desai and J.T. Christian eds., McGraw-Hill.

Mitchell, P.W. (1980), The Structural Analysis of Footings on Expansive Soil, *Kenneth W.G. Smith & Associates*, Research Report No. 1, 2nd edn..

Richards, B.G. (1967), 'Moisture Flow and Equilibria in Unsaturated Soils for Shallow Foundations', *ASTM Symp., Permeability and Capillarity*, ASTM, STP 417, pp. 4-34.

Sokolov, M. and Amir, J. M. (1973), 'Moisture Distribution in Covered Clays', *Proc. 3th Int. Conf. on Expansive Soils*, Israel, pp. 129-136.

Wray, W.K. (1980), 'Analysis of Stiffened Slabs-on-Ground over Expansive Soils', *Proc. 4th Int. Conf. Expansive Soils*, Denver, USA, pp. 558-581.